Polymerization and Gelation of Actin Studied by Fluorescence Photobleaching Recovery†

Jonathan F. Tait and Carl Frieden*

ABSTRACT: The polymerization of rabbit skeletal muscle actin was studied with the technique of fluorescence photobleaching recovery by using trace amounts (5%) of actin labeled with (iodoacetamido)tetramethylrhodamine as the fluorescent probe. This derivative's fluorescence increases 50% upon polymerization, so the rate and extent of polymer formation can be measured from the same sample used in the photobleaching experiment. When photobleaching experiments are done under conditions suitable for following the diffusion of polymeric actin, the progress of polymerization at 1 mg/mL and 2 mM Mg^{2+} is as follows: (1) Prior to significant accumulation of polymer, all the actin diffuses too rapidly to be observed. (2) As polymer forms, it diffuses with an apparent diffusion coefficient in the range of ($\sim$0.05–0.5) $\times$ 10^{-8} cm^2/s. (3) Before completion of polymerization, filaments become immobilized (apparent diffusion coefficient $\ll 2 \times 10^{-11}$ cm^2/s). The second stage probably represents growing polymers whose diffusion is hindered by interaction with other polymers; the third stage is attributed to immobilization of filaments in networks. Immobilization can be reversed by shearing the sample, but the filaments become immobile again within 3–5 min under these conditions. Immobilization occurs at a lower concentration of F-actin when the total actin concentration is reduced at constant Mg^{2+} concentration or when actin is polymerized with KCl rather than Mg^{2+}. These results suggest that filaments are longer under conditions where the rate of polymerization is slow. Polymerization in the presence of cytochalasin D (2 μM) delays the onset of immobilization until after a steady-state concentration of F-actin is reached, indicating that filaments grown in the presence of cytochalasin are initially short but gradually lengthen. Polymerized actin (1 mg/mL, 2 mM Mg^{2+}) almost completely prevents the diffusion of 250-nm fluorescent beads, suggesting that the effective pore size of the actin network is less than 250 nm. We conclude that fluorescence photobleaching recovery experiments can measure relative sizes of actin filaments, filament annealing, and network formation.

Monomeric actin polymerizes into long rodlike molecules, a process that has been intensively studied in vitro (Oosawa & Asakura, 1975). Polymerization of actin may also be involved in cellular processes such as endocytosis, motility, and the gelation of cytoplasm (Clarke & Spudich, 1977). Several recently discovered proteins could control these events by altering the rate or extent of polymerization, the length of the polymers, or the propensity of filaments to form networks (Schliwa, 1981). The properties of actin polymers have been studied by several techniques, including electron microscopy (Kawamura & Maruyama, 1970), flow birefringence (Maruyama, 1964), and quasi-elastic light scattering (Fujime & Ishiwata, 1971; Carlson & Fraser, 1974); networks of actin filaments have been investigated by low-shear viscometry (MacLean-Fletcher & Pollard, 1980a; Maruyama et al., 1974) and viscoelasticity measurements (Maruyama et al., 1974). These techniques generally require that solutions be sheared (except in light scattering), which can disrupt networks and filaments. Furthermore, most cannot be applied to living cells. Fluorescence photobleaching recovery (FPR)[1] (Koppel et al., 1976) is a technique that could overcome these limitations because it can be applied on a microscopic scale without shearing the sample under study. Lanni et al. (1981) recently studied actin polymerization in FPR. They used conditions suitable for following the diffusion of monomeric actin and found that FPR can measure the relative amounts of monomeric and polymeric actin in vitro. We will show here that FPR can also measure several other properties of actin, including relative filament sizes and network formation, if one uses conditions suitable for following the diffusion of polymeric actin.

FPR can be used to determine the diffusion coefficients of fluorescent molecules. This is accomplished by destroying a fraction of the fluorescent molecules in a defined region with a brief pulse of intense light. Unbleached molecules then diffuse into the bleached region from the surrounding area, and this process is monitored by measuring the return of the fluorescence with an attenuated beam. The time course of fluorescence recovery gives a measure of the diffusion coefficient and the extent of recovery indicates what fraction of the fluorescent molecules do not diffuse on the experimental time scale.

In this report, we describe the results of an FPR study of the polymerization of actin. We have used trace amounts of actin labeled with rhodamine at Cys-373; since the fluorescence of this derivative increases $\sim$1.5-fold upon polymerization (Tait & Frieden, 1982), the results of the photobleaching experiments can be checked by a simultaneous, independent measure of the overall rate and extent of polymerization. We show that FPR can detect several stages in the polymerization process. Also, the diffusion of F-actin under most conditions is at least 2 orders of magnitude slower than would be expected from previous evidence (Fujime, 1970; Carlson & Fraser, 1974), which suggests immobilization of filaments in network structures. Finally, filaments formed in the presence of cytochalasin D are initially fully mobile, but after polymerization is complete, they gradually form longer filaments which are

† From the Department of Biological Chemistry, Division of Biology and Biomedical Sciences, Washington University School of Medicine, St. Louis, Missouri 63110. *Received December 22, 1981.* Supported by National Institutes of Health Grant AM 13332 and Medical Scientist Grant GM 07200.

[1] Abbreviations: FPR, fluorescence photobleaching recovery; rhodamine–actin, actin labeled with (iodoacetamido)tetramethylrhodamine; t_d, characteristic time of recovery due to diffusion; $NaDodSO_4$, sodium dodecyl sulfate; ATP, adenosine 5′-triphosphate; Tris, tris(hydroxymethyl)aminomethane.

0006-2960/82/0421-3666$01.25/0

partially immobilized in networks.

Materials and Methods

Materials. The procedures for preparation, storage, and quantification of actin and rhodamine–actin are described elsewhere (Tait & Frieden, 1982). These include gel filtration of actin on Sephacryl S-300 as the final purification step and centrifugation of all actin solutions just prior to use. The gel filtration step removes contaminants that reduce the low-shear viscosity of F-actin (MacLean-Fletcher & Pollard, 1980b). The actin was greater than 99% pure as judged by NaDodSO$_4$–polyacrylamide gel electrophoresis. Rhodamine–actin and unlabeled actin were mixed to give a final labeling ratio of 5% ($\epsilon_{554} = 2.3 \times 10^4$ M^{-1} cm^{-1} (Tait & Frieden, 1982)). The standard buffer contained 0.2 mM $CaCl_2$, 0.2 mM Na_2ATP, 1.5 mM NaN_3, and 2 mM Tris-HCl, pH 8.0 at 25 °C. Fluorescently labeled latex beads were from Polysciences, Inc., Warrington, PA (product no. 9834). Cytochalasin D was from Aldrich. FPR studies were done in rectangular glass capillaries (0.3-mm path length, 3 mm wide, 50 mm long), which were used as supplied (microslides, from Vitro Dynamics, Rockaway, NJ). The characteristics of polymerization were the same in silanized capillaries.

FPR Apparatus. The FPR apparatus is a modified version (N. O. Petersen, W. B. McConnaughey and E. L. Elson, unpublished results) of the design of Koppel et al. (1976). Laser light (514.5 nm) is focused on the sample via a dichroic mirror in a modified fluorescence microscope. The microscope also collects fluorescence from the sample and channels it via a barrier filter (OG550, Schott, Duryea, PA) and a pinhole diaphragm to a photomultiplier. The sample is bleached by transiently increasing the beam intensity by $\sim 10^4$. (The power of the observation beam was estimated from the laser power monitor, with attenuation of $\sim 10^4$ for the bleach shutter, ~ 2 for other optical losses, and a variable factor for any neutral density filters in the beam path.) All experiments were done with a 40× microscope objective (Zeiss Neofluar, numerical aperture 0.75), which gives a Gaussian beam radius, w, of 1.8 μm [determined as described by N. O. Petersen, W. B. McConnaughey, and E. L. Elson (unpublished results)]. The beam diameter can be increased by placing a lens in the beam path. Background fluorescence was <5% of total fluorescence. Under our conditions the observed region of solution can be approximated by a cylinder, so the kinetics of recovery can be described by the equations of Axelrod et al. (1976). Using Icenogle's (1981) formulas for calculating the effective path length from which fluorescence is collected, we obtain a value of 19 μm for the 40× objective/0.4-mm pinhole combination. This is far less than the depth of the slide (300 μm), so effects due to the capillary wall (e.g., adsorption) do not contribute to the results.

Measurement of Diffusion of G-Actin. FPR studies of monomeric actin were done in the standard buffer with actin containing trace amounts of rhodamine–actin. The Gaussian beam radius was 4.5 μm, and the observation beam power was ~7 μW. Data were collected as the sum of 32 consecutive bleaches on the same spot (20-ms bleach, 2-s record), with a 10-s wait between bleaches to allow full recovery.

Procedure for Following Time Course of Polymerization. Samples were prepared in polypropylene tubes just before use (50-μL final volume). At time zero, the polymerizing agent (a concentrated solution of $MgSO_4$ or KCl) was added; the sample was mixed by drawing it up 3 times with a micropipet. The sample was then injected into a capillary mounted on the microscope stage (temperature 21–23 °C). The microscope had already been focused to the approximate center of the capillary, allowing measurements to begin 15–30 s after addition of Mg^{2+} or KCl. Data records (see Figure 1) were usually 41 s long: ~4 s for the prebleach base line, 0.1–0.8 s for the bleach itself, and ~36 s for the recovery measurement. For data presented in the figures, the time at the beginning of the record was considered to be the time of the measurement. F-Actin concentrations during polymerization were calculated from the fluorescence enhancement by assuming a maximum enhancement of 0.55 (i.e., 1.55-fold) if all the actin were polymerized. Each bleach was performed on a section of the slide not previously exposed to the laser beam to obtain a proper measure of the proportion of immobile material present. The power of the observation beam was kept low enough so that less than 5% of any immobile fluorophore would be bleached by the observation beam in 40 s. Although the rate of polymerization was somewhat faster in the FPR capillary than in a standard 3-mL quartz fluorometer cell [see Tait & Frieden (1982)], this difference was not due to photobleaching (see Results). We have seen a similar rate acceleration for polymerization carried out in 0.2-mL quartz fluorometer microcells, so these differences are not intrinsic to FPR experiments. In addition, we could always measure the rate of polymerization in the FPR cell by using rhodamine–actin's fluorescence enhancement, thereby avoiding potentially misleading comparisons with measurements made under different conditions with a different technique.

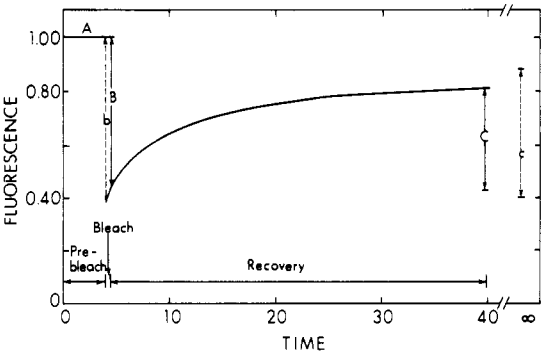

FIGURE 1: Definition of terms used to describe FPR data. The figure shows the recovery expected for diffusion with $t_d = 5$ s and a mobile fraction of 0.8. Terms: A, prebleach fluorescence; B, amount bleached; b, amount bleached, extrapolated to start to bleach; C/B, percent recovery; c/b, mobile fraction, extrapolated to infinite time.

Data Analysis. Figure 1 defines the terms we will use to describe FPR data. The prebleach fluorescence intensity (A in Figure 1) is recorded during the prebleach period. Some fluorophore is then destroyed during the bleach period. During the recovery period, the fluorescence intensity increases as unbleached fluoropohore enters the bleached region. When the recovery of fluorescence is due to diffusion, the kinetics of recovery can be described by an equation with two parameters (Axelrod et al., 1976): the "amount" of bleaching, extrapolated to the beginning of the bleach period (distance b in Figure 1), and the characteristic time of the recovery, t_d. (For small amounts of bleaching, t_d is approximately equal to the half-time for fluorescence recovery.) The diffusion coefficient of the fluorophore, D, is related to t_d and the Gaussian beam radius, w, by the expression (Axelrod et al., 1976)

$$D = w^2/(4t_d)$$

This analysis is usually modified to include a third parameter, the mobile fraction (c/b in Figure 1), which allows for any fluorophore that diffuses too slowly to be observed on the chosen time scale. The mobile fraction is obtained by extrapolating the observed recovery to infinite time.

This analysis can be directly applied to determine the diffusion coefficient of monomeric actin, but application to F-actin is more complex for several reasons. First, F-actin is polydisperse (Kawamura & Maruyama, 1970); the calculated diffusion coefficient is therefore only an average value. Second, we show here that under many circumstances only a small fraction of the F-actin is free to diffuse, so the recovery time and mobile fraction often cannot be defined precisely by the curve-fitting procedure. Third, when recovery from bleaching is measured during polymerization, there is a small component of fluorescence increase due to rhodamine–actin's fluorescence enhancement upon polymerization, which complicates precise calculation of t_d and the mobile fraction. Finally, low levels of fluorescence limit the precision of single records obtained sequentially during polymerization. For these reasons, t_d values calculated for F-actin are relatively rough guides to filament size rather than well-defined measures of diffusion coefficients.

Values of t_d were calculated from FPR data by applying a nonlinear least-squares curve-fitting procedure [program CURFIT in Bevington (1969)] to the equation describing diffusive recovery from bleaching. [The first 16 terms of the series solution were used (Axelrod et al., 1976), with an additional term representing the mobile fraction.] Estimated standard deviations of the parameters from each fit were calculated as described (Bevington, 1969) to provide minimal estimates of uncertainties.

The curve-fitting procedure was often not suitable for F-actin for the reasons given. We therefore estimated the amount of bleaching from the fluorescence level directly after the bleach period (B in Figure 1) and the mobile fraction from the fluorescence level at the end of the recovery period. We refer to this value as "percent recovery" (C/B in Figure 1) to distinguish it from "mobile fraction" (c/b in Figure 1). The percent recovery was usually adequate as an estimate of the mobile fraction because either recoveries were rapid (hence nearly complete by the end of the recovery period) or the extent of recovery was very small.

Percent recovery values were corrected for fluorescence enhancement due to further polymerization during the recovery period by using consecutive prebleach fluorescence levels to estimate the rate of fluorescence increase due to polymerization. This rate was multiplied by the length of the recovery period (e.g., 35 s) and subtracted from the fluorescence at the end of the recovery period. The correction is small except at the beginning of polymerization, when the amount bleached is slight, or when polymerization is very rapid. The correction procedure assumes that the rate of polymerization in the bleached region is the same as that in the bulk solution, which is justified for several reasons. The concentration of fluorescent monomer is the same in the bleached region as elsewhere due to its rapid diffusion (t_d = 15 ms), and the concentration of polymer is also the same (only the fluorophores, not the entire polymer, were destroyed by bleaching). The polymerization reaction is also not accelerated by the bleaching pulse, as we will show.

Results

Diffusion of G-Actin. We obtained a diffusion coefficient of 5.7×10^{-7} cm^2/s for monomeric rhodamine–actin (23 °C, 2 mM Tris, pH 8, 0.2 mM $CaCl_2$, 0.2 mM ATP, 1.5 mM NaN_3, and 0.8 mg/mL actin). This agrees reasonably well with Mihashi's (1964) value of 5.3×10^{-7} cm^2/s for ADP–G-actin and Lanni et al.'s (1981) value of $(4.9–6.1) \times 10^{-7}$ cm^2/s for fluorescein-labeled G-actin. The diffusion of monomeric actin is therefore rapid and will not be observed in the subsequent experiments, which are designed to measure much slower rates of diffusion. (Any oligomeric nuclei would also not be detected, even if their concentration were measurable, since they would diffuse almost as rapidly as G-actin.)

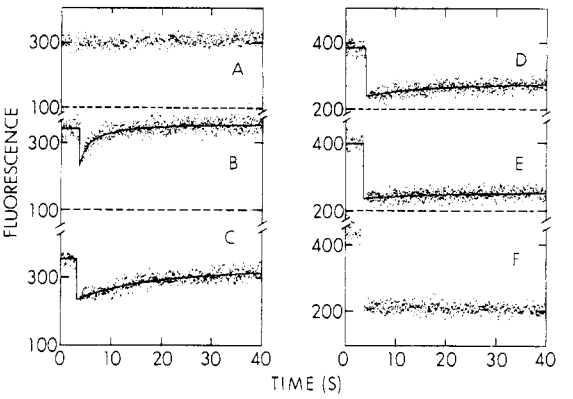

FIGURE 2: Selected FPR traces showing transformation of G-actin into F-actin. Actin (1 mg/mL, 5% rhodamine–actin) was polymerized with 2 mM $MgSO_4$ (22 °C, pH 8, 2 mM Tris-HCl, 0.2 mM ATP, 0.2 mM $CaCl_2$, and 1.5 mM NaN_3). The laser power was 0.1 μW and the bleach duration 400 ms; fluorescence intensity is in counts/40 ms. Records were begun at the following times (minutes) after addition of Mg^{2+}: (A) 0.7, (B) 2.2, (C) 3.1, (D) 4.1, (E) 5.3, and (F) 30. Fluorescence enhancements were calculated from the ratio of prebleach fluorescence to the prebleach fluorescence of record A and are as follows: (A) 0.00, (B) 0.16, (C) 0.20, (D) 0.30, (E) 0.34, and (F) 0.49. The solid lines in panels B–E are the best fit of the data to the equation describing diffusive recovery from bleaching.

Polymerization of Trace-Labeled Actin. FPR studies of the polymerization reaction were done with unlabeled actin containing trace quantities (5%) of rhodamine–actin. The fluorescence of rhodamine–actin increases by approximately 50% upon polymerization, and the time course of fluorescence change is a measure of the rate of incorporation of monomer into polymer (Tait & Frieden, 1982). The progress of polymerization in the FPR sample can thus be measured from consecutive prebleach fluorescence levels (see Figure 1).

Figure 2 shows the results obtained when FPR measurements are made sequentially during polymerization at 1 mg/mL and 2 mM Mg^{2+}. At an early stage of polymerization (Figure 2A; 0.7 min after addition of Mg^{2+}), recovery from bleaching is essentially instantaneous. This reflects the rapid diffusion of monomeric actin (t_d = 15 ms) and the lack of any appreciable polymer at this time. By 2 min (Figure 2B), some polymer has accumulated, and a recovery can be measured with a t_d of 2 ± 0.3 s. One minute later (Figure 2C), the amount of bleaching has increased, and the characteristic recovery time has lengthened (t_d = 17 ± 3 s). At 4 min (Figure 2D), a substantial fraction of the actin does not recover on this time scale (t_d = 14 ± 5 s, percent recovery = 20). The trend to immobility is even more pronounced in Figure 2E, where the t_d value (16 ± 11 s) can no longer be accurately determined given the slight degree of recovery. At longer times (Figure 2F), there is no further change except an increase in the amount of bleaching. If fluorescence is recorded for a longer time after the bleach, there is still no recovery at this stage of polymerization (percent recovery ~0 at 400 s). This puts a lower limit of at least ~500 s on the t_d under these conditions, corresponding to an upper limit of $\sim 2 \times 10^{-11}$ cm^2/s on the apparent diffusion coefficient of fully polymerized F-actin at 1 mg/mL in 2 mM Mg^{2+}.

The fluorescence enhancement [Figure 3 (●)] and the amount bleached [Figure 3 (■)] increase at roughly the same rate during polymerization. (Data were replotted from Figure 2.) This suggests that the amount bleached measures only polymeric actin. (Because monomeric actin diffuses so rapidly,

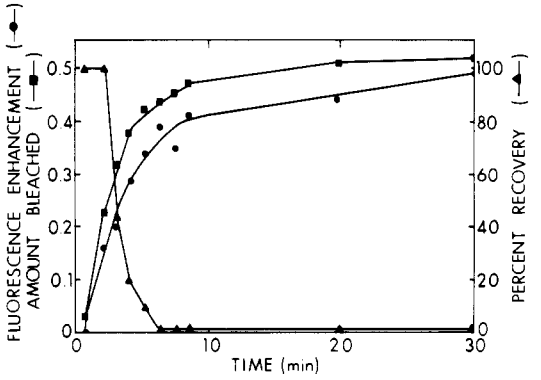

FIGURE 3: Time course of fluorescence enhancement (●), amount bleached (■), and percent recovery (▲) for polymerization at 1 mg/mL and 2 mM Mg^{2+}. Data are from the experiment described in Figure 2.

its bleaching does not contribute to the measured amount bleached.) There is also a close correlation between fluorescence enhancement and amount bleached under the other conditions that we have studied.

The percent recovery [Figure 3 (▲)] drops rapidly to zero well before the end of the polymerization reaction. This indicates that early in the reaction polymer is free to diffuse but at a certain point the polymer becomes immobile (unable to diffuse), and this immobility persists as polymerization goes to completion. The cause of this immobility is probably formation of networks of actin filaments (see Discussion).

The fluorescence enhancement due to polymerization itself makes a relatively small contribution to the observed recoveries after bleaching. The rate of fluorescence enhancement is never more than ~0.05/35 s (Figure 3), so that the observed recoveries (e.g., Figure 2B,C) primarily represent diffusion rather than de novo polymerization. This effect becomes even less important at slower rates of polymerization.

Lanni et al. (1981) suggested that photobleaching may accelerate the polymerization of actin. We have not seen this phenomenon in our experiments. The time course of fluorescence enhancement in the FPR cell is the same when no bleaches are performed during polymerization. The rates of polymerization and immobilization are also unchanged when the bleach duration is varied from 100 to 3000 ms. The chosen level of labeling (5% of monomers labeled with rhodamine) does not alter the observed phases of polymerization, since results are the same at a 10-fold lower labeling ratio. Nor have we seen anomalous recoveries above base line when multiple bleaches are done in the same location [which is what Lanni et al. (1981) observed]. Thus, although we cannot rule out the possibility of photoinduced effects, they do not seem to contribute to our results.

Effect of F-Actin on Diffusion of Other Molecules. We followed diffusion on the time scale of G-actin during polymerization at 1 mg/mL and 1.5 mM Mg^{2+} and found that t_d values stayed constant within a factor of 2, in agreement with Lanni et al. (1981), until the recovery could no longer be accurately defined due to the small quantity of G-actin remaining. We also followed the diffusion of rhodamine-labeled insulin (as separate A and B chains) in the presence of unlabeled actin; the insulin's diffusion was also unaffected by the polymerization of actin. Although these data are not precise enough to reveal subtle effects of actin polymers on the diffusion of small proteins, they do show that the diffusion of G-actin in F-actin solutions is unhindered and is far too rapid to account for the recoveries seen in Figure 2. However, diffusion of much larger molecules is hindered by polymerization of actin. We measured the diffusion of fluorescent carboxylated microspheres (250 nm in diameter) in solutions of G-actin and F-actin (1 mg/mL, polymerized with 2 mM Mg^{2+}). As shown in Figure 4, the beads are completely mobile in G-actin but become largely (~80%) immobilized in F-actin. [The observed slight recovery in F-actin could represent localized movement of beads over distances less than the beam radius. Immobilization is not due to adherence of beads to F-actin because it does not occur at a lower actin concentration (0.5 mg/mL).] Although other interpretations are possible, these results suggest that the effective pore size of an F-actin network is less than 250 nm at 1 mg/mL and 2 mM Mg^{2+}.

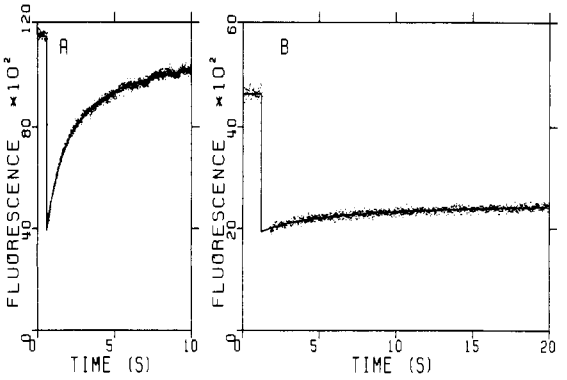

FIGURE 4: Diffusion of latex spheres (diameter = 250 ± 3 nm) in solutions of G-actin and F-actin. (A) Diffusion in G-actin (1 mg/mL). Sum of 40 individual records (laser power 2 μW, 40-ms bleach). The fitted curve (solid line) has t_d = 1.2 ± 0.1 s and mobile fraction (extrapolated to infinite time) = 0.95. The slight fluctuations in the data reflect concentration fluctuations due to the small number of spheres in the illuminated volume. (B) Diffusion in F-actin (1 mg/mL, 2 mM Mg^{2+}). Sum of 40 individual bleaches recorded 220 min after addition of Mg^{2+} (laser power 0.2 μW, 400-ms bleach). The curve-fitting procedure gives t_d = 4.0 ± 0.3 s and mobile fraction (extrapolated to infinite time) = 0.22. The mobile fraction is essentially the same (0.25) if recovery is followed for 100 s rather than 20 s.

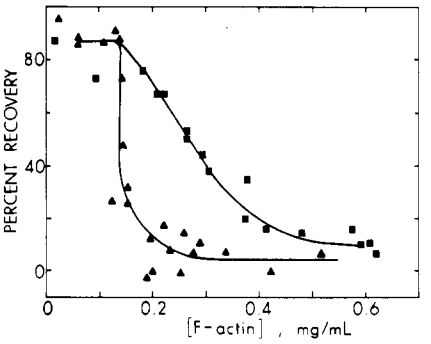

FIGURE 5: Percent recovery vs. F-actin concentration under conditions that give different rates of polymerization. Actin (1 mg/mL) was polymerized at 23 °C with 1 mM $MgSO_4$ (■) or 100 mM KCl (▲). Other experimental conditions were as in Figure 2. (The polymerization rate is faster with 1 mM $MgSO_4$ than with 100 mM KCl.) Lines are arbitrary curves to show trends in the data. The laser power was 0.1 μW; the bleach duration was 800 ms for the 1 mM $MgSO_4$ sample and 400 ms for the 100 mM KCl sample. The concentration of F-actin was calculated from the fluorescence enhancement by assuming a maximal enhancement of 0.55 if all the actin were polymerized.

Effect of Polymerization Conditions on Immobilization. When polymerization is followed under different conditions than in Figure 2, the same general pattern is seen. However, immobilization occurs at different concentrations of F-actin depending on the conditions used to induce polymerization. In Figure 5, the total actin concentration is the same (1 mg/mL) for both samples, but immobilization occurs at a lower concentration of F-actin for the sample polymerized with

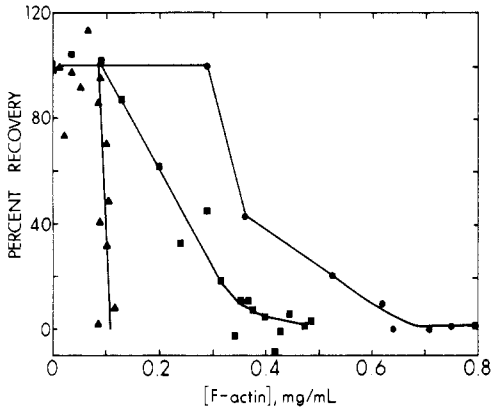

FIGURE 6: Percent recovery vs. F-actin concentration for polymerization at three different actin concentrations. Actin at a total concentration of 1 (●), 0.5 (■), or 0.25 mg/mL (▲) was polymerized with 2 mM $MgSO_4$ at 22 °C. Lines are arbitrary curves to show general trends in the data. The laser power was 0.1 μW, and the bleaches were 400 ms. The F-actin concentration was calculated from the fluorescence enhancement. Values for the 0.25 mg/mL sample were averaged in groups of three due to their low fluorescence level. Data for 1 mg/mL were replotted from Figure 3.

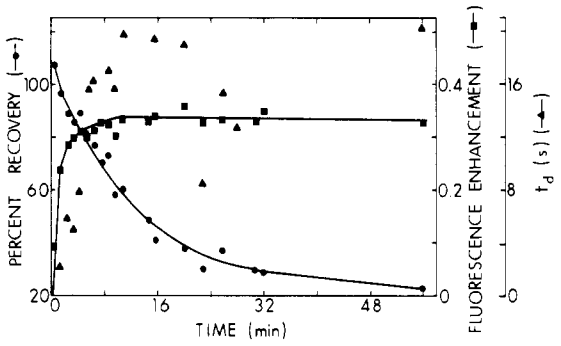

FIGURE 7: Polymerization of actin (1 mg/mL, 2 mM $MgSO_4$) in the presence of 2 μM cytochalasin D. Fluorescence enhancement (■), percent recovery (●), and t_d (▲) are plotted against time elapsed since addition of Mg^{2+}. The fluorescence enhancement is calculated relative to a sample not containing Mg^{2+}. The lines are arbitrary curves drawn to illustrate general trends in the data. The laser power was 0.2 μW, and the bleach duration was 600 ms. Controls containing the solvent for the cytochalasin (*N,N*-dimethylformamide, 0.1% v/v) were identical with samples without the solvent. Percent recovery values at later times are 10–30% less than corresponding values of the mobile fraction extrapolated to infinite time due to the relatively large t_d values. However, both parameters show exactly the same downward trend with time.

100 mM KCl (▲) than for the sample with 1 mM Mg^{2+} (■). The transition to immobility also occurs over a narrower range of F-actin concentrations for the KCl-polymerized sample. Since polymerization (measured by fluorescence enhancement) is slower in the presence of 100 mM KCl than in the presence of 1 mM Mg^{2+}, these differences may be due to differing polymerization rates as well as to differences in ionic conditions. This seems likely because immobilization also occurs at different F-actin concentrations when the rate of polymerization is altered by changing the Mg^{2+} concentration, occurring at higher F-actin concentrations at higher Mg^{2+} concentrations [e.g., 2 mM; Figure 6 (●)] and at lower F-actin concentrations at lower Mg^{2+} concentrations [e.g., 0.5 mM (not shown)]. In addition, immobilization occurs at a higher F-actin concentration when polymerization (1 mg/mL, 1 mM Mg^{2+}) is accelerated by the presence of F-actin fragments. Thus it seems likely that the rate of polymerization, as well as ionic conditions, affects the concentration of F-actin at which immobilization first occurs during polymerization.

A similar effect is observed when the actin concentration is varied (Figure 6). Here actin is polymerized with 2 mM Mg^{2+} at total concentrations of 1 (●), 0.5 (■), and 0.25 mg/mL (▲). The rate of polymerization decreases as the actin concentration decreases, and there is a corresponding drop in the concentration of F-actin at which immobilization occurs. For example, the sample containing 0.25 mg/mL total actin is fully immobilized when the F-actin concentration reaches ~0.1 mg/mL; the samples with higher total actin concentrations are still fully mobile at this concentration of F-actin. These results probably reflect increased filament size at slower rates of polymerization (see Discussion).

Partial Mobility at a Very Low Actin Concentration. If immobilization represents formation of networks from preformed filaments, these interactions might be lessened or prevented at low concentrations of F-actin. When actin is polymerized with 2 mM Mg^{2+} at a concentration of 0.05 mg/mL, after 11 h the percent recovery is 75 and the t_d is 7 ± 0.7 s; there is little further change after 21 h (percent recovery = 61, t_d = 8 ± 1.2 s). These results suggest that immobilization (and hence network formation) is only partial at low concentrations of F-actin (~0.02 mg/mL under these conditions). Nevertheless, the polymer that does diffuse probably still interacts with other filaments because its apparent diffusion coefficient (1×10^{-9} cm^2/s) is 5–10-fold less than would be expected for a rodlike molecule 3–6 μm long. (This discrepancy will be analyzed further under Discussion.)

Effect of Cytochalasin D. Evidence from electron microscopy (Hartwig & Stossel, 1979) and flow birefringence (Maruyama et al., 1980) suggests that cytochalasin shortens actin filaments. Our results are consistent with these previous studies. When polymerization is followed at 1 mg/mL, 2 mM Mg^{2+}, and 2 μM cytochalasin D (Figure 7), recovery times are initially shorter than those in the absence of cytochalasin. For example, t_d is 2 ± 0.2 s at an F-actin concentration of 0.44 mg/mL (calculated from the fluorescence enhancement) in the presence of 2 μM cytochalasin D (Figure 7) but is 17 ± 3 s at a concentration of 0.36 mg/mL in the absence of cytochalasin (Figure 2C). The percent recovery is also initially higher in the presence of cytochalasin.

These data (Figure 7) also show a phenomenon that was not expected from previous work: the effect of cytochalasin on filament size gradually wanes after the steady-state concentration of F-actin is established. The formation of F-actin is 90% complete by 3 min, but after this time the t_d values increase and the percent recovery gradually declines. These results suggest that the presence of cytochalasin D at 2 μM during polymerization initially results in a population of many short filaments, which then gradually form fewer longer filaments.

Rate of Filament Annealing after Shearing. Small fragments of F-actin are able to anneal into larger polymers, but this process is difficult to measure because few techniques are sensitive to filament size. Kawamura & Maruyama's (1970) electron microscopic study showed that the initial increase in filament length after sonication was rapid (occurring within a few minutes), but the filaments did not return to the control length until 12 h after sonication. We have performed initial investigations of filament annealing by shearing polymerized actin samples and then examining them by FPR. Application of a shear gradient of ~100 s^{-1} caused previously immobile actin to become completely mobile (Tait & Frieden, 1982). We have followed the time course of recovery from shearing by doing successive bleaches after the sample is sheared. F-Actin usually returns to its fully immobile state within 3–5 min after shearing at 1 mg/mL and 1.5 mM Mg^{2+} (data not

shown). The shearing procedure almost certainly breaks existing filaments as well as networks, because if a sample is sheared in the capillary before the completion of polymerization, the subsequent rate of polymerization is increased relative to an unsheared control. The acceleration of polymerization indicates the presence of filament fragments that act as nuclei for further polymerization. Although further work is necessary with an improved method for generating reproducible shear stresses, these results show that both the initial stages of filament reannealing and network formation occur rapidly after disruption of filaments.

Discussion

This study has defined some of the major features of the polymerization of actin that can be observed by the technique of fluorescence photobleaching recovery. Because these experiments were done on a time scale commensurate with the diffusion of polymeric rather than monomeric actin, we have detected several properties of the polymerization reaction that were not observed in a previous FPR study of actin polymerization (Lanni et al., 1981). When polymerization is followed at 1 mg/mL and 2 mM Mg^{2+}, several phases are seen: (1) an initial period in which fluorophore diffuses with a characteristic time similar to that of monomeric actin, (2) a phase with full to partial recovery characterized by apparent diffusion coefficients in the range of ($\sim$0.05–0.5) $\times$ 10^{-8} cm^2/s, and (3) a final phase, occurring well before the completion of the reaction, in which F-actin is essentially immobile (apparent diffusion coefficient $\ll 2 \times 10^{-11}$ cm^2/s). The immobilization of the filaments occurs at an earlier fractional extent of polymerization under conditions giving slower polymerization rates. Immobilization can be delayed by cytochalasin D and can be partially prevented by polymerizing at extremely low concentrations of actin (0.05 mg/mL). We believe these results can be best explained by attributing immobilization to the formation of polymer networks: with an indefinitely large molecular weight, a network has an indefinitely small macroscopic translational diffusion coefficient. Accordingly, we will first consider what experimental and theoretical evidence bears on this interpretation.

Diffusion of F-Actin. The expected diffusion coefficient of F-actin can be calculated by considering F-actin as a rod with a width of 8 nm and a length of $\sim$2.7 nm per monomer (Hanson & Lowy, 1963). The persistence length of F-actin is between 6 and 25 μm (Oosawa, 1980), so below this value the filament can be treated as a rigid rod. The diffusion coefficient is then calculated from the frictional coefficient of an equivalent prolate ellipsoid (Tanford, 1961) or an equivalent cylinder (Garcia de la Torre & Bloomfield, 1981). Both methods give $D_{20,w}$ (orientationally averaged) = 1.0 $\times$ 10^{-8} cm^2/s (corresponding to a t_d of 0.8 s) for a 1000-subunit (2.7-μm) filament, in agreement with Fujime's (1970) estimate. For diffusion parallel to the molecule's long axis, $D_{20,w}$ = 1.3 $\times$ 10^{-8} cm^2/s; perpendicular to the long axis, $D_{20,w}$ = 0.8 $\times$ 10^{-8} cm^2/s. The diffusion coefficient will vary approximately as length$^{-0.8}$ (Tanford, 1961).

The calculated diffusion coefficient is clearly far larger than what we have measured for fully polymerized actin. Although the weight-average filament length may well be larger than $\sim$3 μm under some conditions (Kawamura & Maruyama, 1970; Hartwig & Stossel, 1979), increased length alone could not explain the discrepancy because of the weak dependence of the diffusion coefficient on length. Interactions between filaments are a more likely cause of slow diffusion. The diffusion of individual filaments could be hindered by transient interactions with other filaments, or individual filaments could be cross-linked into large assemblages that diffuse slowly if at all. The first explanation is not likely for several reasons. First, physical considerations indicate that translational diffusion of a thin rodlike molecule parallel to its long axis is essentially unhindered, even in concentrated solutions where rotational diffusion and translational diffusion perpendicular to the long axis would be quite hindered.[2] There is experimental evidence from several systems that supports this analysis. The measured translational diffusion coefficient of fd virus is the same as the value calculated from its known dimensions (900 $\times$ 8 nm by electron microscopy) and is nearly independent of concentration from 0.07 to 1.4 mg/mL despite the fact that the average interparticle distance is less than the particle length above 0.03 mg/mL (Newman et al., 1977). Likewise, native muscle thin filaments (1000 nm long) have a translational diffusion coefficient that agrees with the calculated value and is independent of concentration from 0.08 to 1.3 mg/mL (Newman & Carlson, 1980). And Lee et al. (1977) have shown good qualitative agreement between a simple model that only allows translational diffusion parallel to the molecule's long axis and experimental results from light scattering studies of large DNA molecules (M_r $\sim$30 $\times$ 10^6). Therefore, although the average interfilament distance [$\sim$0.3 μm at 1 mg/mL (Fujime & Ishiwata, 1971)] is much less than the filament length, we conclude that random collisions between actin filaments could not explain the extreme reduction (>1000-fold) in the rate of translational diffusion that we have seen in this study.

The observed slow diffusion of F-actin under most conditions we studied is therefore likely to be due to cross-links between individual filaments that are permanent on the time scale of recovery from bleaching. If individual filaments become cross-linked to other filaments, they will diffuse at slower rates characteristic of assemblages of polymers. The cross-linking process culminates in the formation of infinite networks (see later), which are completely unable to diffuse.

These considerations can explain the phases of polymerization we have observed. Early in polymerization, both the concentration of F-actin and its average molecular weight are low—both factors that minimize the hindrances to diffusion. As polymerization proceeds, the F-actin concentration and the average filament length both increase, and along with them the potential for cross-linking. Thus the apparent diffusion coefficient of the F-actin is expected to decline over the course of polymerization—in agreement with our results showing rising t_d values during polymerization.

There have been several studies of F-actin by quasi-elastic light scattering, another technique that does not shear solutions. These studies seem to disagree with ours because they obtained much larger values of the apparent translational diffusion coefficient [in the range of 0.3 $\times$ 10^{-8} cm^2/s (Fujime, 1970) to 1 $\times$ 10^{-8} cm^2/s (Carlson & Fraser, 1974)]. However, the determination of a translational diffusion coefficient from light scattering data is not straightforward for a molecule as large as F-actin. Rotational diffusion and internal motions, in ad-

[2] We can estimate the magnitude of this effect in the FPR experiments if we assume that F-actin molecules are randomly oriented and can only diffuse parallel to their long axes on the time scale we have studied. The rate of fluorescence recovery due to molecules at an angle θ with respect to a plane perpendicular to the laser beam's axis of propagation would then be proportional to $\cos^2 \theta$; this is because a distance X along the filament's axis corresponds to a distance $X \cos \theta$ relative to the beam axis and because the time required for diffusion goes up with the square of the distance. Thus at most angles the rate of fluorescence recovery is not drastically less than would be predicted from the value of the translational diffusion coefficient parallel to the molecule's long axis (for example, at θ = 60°, $\cos^2 \theta$ is 0.25).

dition to translational diffusion, contribute to the fluctuations in scattered light. Current light scattering theory is also inadequate to deal with the nature of gels and entangled solutions of polymers (Bloomfield, 1981). More recent reports have emphasized the theoretical and experimental difficulties encountered in quasi-elastic light scattering studies of F-actin (Maeda & Fujime, 1977; Newman & Carlson, 1980) and microtubules (Gethner & Gaskin, 1978). Different procedures for preparing actin could also contribute to differences between our study and previous ones. Finally, there is a difference in the range of motion detected by light scattering compared to that by FPR: fluctuations in scattered light will occur if the molecule moves about half a wavelength of light ($\sim$0.3 μm), whereas fluorescence recovery requires movement over approximately the beam radius ($\geq$1.8 μm in this study).

In conclusion, we believe that FPR provides a less ambiguous experimental determination of the macroscopic translational diffusion coefficient of F-actin than does quasi-elastic light scattering. Under most conditions F-actin is unable to diffuse at the rate expected theoretically for an individual filament, and its apparent translational diffusion coefficent ($\ll 2 \times 10^{-11}$ cm^2/s) is at least 100 times smaller than previous studies suggested (Fujime, 1970; Carlson & Fraser, 1974).

Nature of Network Formation in Solutions of F-Actin. Rheological studies have suggested the existence of networks of F-actin in solution. The viscosity of F-actin solutions increases without limit as the shear rate decreases, and these solutions have viscoelastic properties consistent with a gel structure; these results differ from those obtained with some other rodlike molecules (e.g., flagella) [see Maruyama et al. (1974) and references cited therein]. But rheological measurements perturb the structure of the gel, and viscosity represents an ill-defined average of the properties of individual filaments and the properties of networks. FPR partially overcomes these problems.

Gelation results from the cross-linking of polymers into an infinite network (Flory, 1953). The transition is characteristically sharp, occurring over a small range of the total extent of the polymerization reaction. When cross-links occur at random, the fraction of cross-linked subunits, ρ_c, required for incipient gelation is reciprocally related to the weight-average degree of polymerization, $\bar{y}_w$: $\rho_c = 1/\bar{y}_w$ (Flory, 1953). This relationship arises from simple statistical considerations: the longer a polymer molecule is, the greater the chance it will be cross-linked to another polymer; at a certain average length, infinite sequences of cross-linked polymers become possible. Gelation occurs suddenly during polymerization because only a slight increase in $\bar{y}_w$ is necessary to cross the threshold into the region allowing gelation.

This analysis can be applied to F-actin if we assume that cross-links represent intermonomer bonds that can occur wherever filaments cross over. (Cross-links could also be due to trace contaminating proteins, but this would not affect the analysis because the contaminant's concentration would be in constant proportion to the actin concentration.) Gelation would then depend on the overall concentration of F-actin (which determines the frequency of crossovers) and on the average filament length (which determines the efficacy of cross-links in promoting infinite networks). The dependence on filament length is probably the stronger of the two, since the distance between filaments would decrease with the cube root of the F-actin concentration.

Under most experimental conditions we have studied, actin filaments eventually become immobile. The observed lack of diffusion is too extreme to reflect transient interactions between filaments; instead, the change from mobile to immobile provides a quantitative measure of network formation. The transition from mobile to immobile polymer occurs at a lower absolute concentration of F-actin and over a smaller increment of polymer concentration under conditions giving lower rates of polymerization (Figures 5 and 6). This can be interpreted as follows: under conditions that favor rapid polymerization, many nuclei are formed, resulting in a larger population of short, growing filaments than during a slower polymerization. When the average filament length reaches its critical value, filament networks form and mobility drops precipitously. Stated another way, in a rapid polymerization the average filament length is smaller at any given extent of polymerization, thus delaying the onset of gelation; also, because there are more growing filaments present in the fast polymerization, a larger change in extent of reaction is required to achieve a given increase in average filament length, accounting for the decreased sharpness of gelation as a function of reaction extent. The average length of filaments goes up as the actin concentration goes down (Kawamura & Karuyama, 1970), in agreement with this interpretation. However, our analysis does not depend on differences in filament length at steady state; only a transient difference in average filament length during the reaction is necessary to explain the results.

At a very low concentration of actin (0.05 mg/mL total actin, $\sim$0.02 mg/mL F-actin), immobilization of filaments is only partial. This probably reflects the concentration dependence of network formation—if the F-actin concentration is low enough, filament crossovers decrease sufficiently that only some filaments are involved in effectively infinite networks.

The rate of polymerization therefore seems to be an important determinant of the concentration of F-actin needed for initial immobilization during polymerization. It is unlikely that cross-linking is the rate-determining step in network formation, since immobilized filaments that are sheared rapidly become immobilized again; also, immobilization occurs at an earlier time (although at a larger F-actin concentration) at faster rates of polymerization. In addition, slow cross-linking is unlikely on purely physical grounds, since a polymer segment can rapidly diffuse over the submicron distances separating it from its neighbors. Ionic conditions are also likely to influence network formation [cf. MacLean-Fletcher & Pollard (1980b)], but they are not the sole determinant of the results in Figures 5 and 6. The concentration of F-actin required for immobilization can be varied by experimental manipulations that alter the rate of polymerization under constant ionic conditions (e.g., variation of the total actin concentration or the addition of F-actin fragments).

Polymerization continues to increase after the transition to immobility is complete (Figures 3, 5, and 6). Why does newly formed polymer apparently not recover after bleaching? Perhaps monomeric actin is primarily adding to preexisting immobile filaments; this is plausible because formation of new nuclei is a cooperative process (Oosawa & Asakura, 1975), which is much less favorable later in the reaction, when the concentration of monomer is low. Also, it would be relatively difficult to detect a low concentration of diffusible polymer against a large background immobile polymer. Alternatively, an existing network may hinder diffusion of a single filament more than the equivalent concentration of un-cross-linked filaments.

Networks of F-actin can also be studied by following the diffusion of other molecules in the presence of F-actin. Our results and those of Lanni et al. (1981) indicate that G-actin's

diffusion is unhindered by F-actin. However, fluorescent latex spheres (250 nm in diameter) become nearly completely immobile in an F-actin solution at 1 mg/mL and 2 mM Mg^{2+} (Figure 4). This suggests that the effective pore size in the network must be less than 250 nm.

Effect of Cytochalasin D. Although cytochalasin is generally thought to inhibit polymerization of actin, several studies have shown that cytochalasin enhances the initial rate of polymerization under some or all conditions (Brenner & Korn, 1980; Dancker & Low, 1979; Howard & Lin, 1979), and it may be more likely that under all conditions cytochalasin D enhances the initial rate of polymerization but decreases the extent (Tellam & Frieden, 1982). This finding suggests that cytochalasin enhances nucleation of actin, perhaps by binding preferentially to nuclei and increasing their steady-state concentration. However, if the cytochalasin molecule bound to a nucleus remains bound as the nucleus grows into a filament, presumably a given filament will elongate less rapidly because cytochalasin blocks its fast-growing end (MacLean-Fletcher & Pollard, 1980c; Pollard & Mooseker, 1981). This model predicts that cytochalasin will reduce average filament size at any particular extent of polymerization. Our data are consistent with this hypothesis, since they show shorter recovery times and larger percent recovery values during polymerization. [Alternatively, cytochalasin could increase the apparent diffusion coefficient by inhibiting filament cross-linking. This seems less likely because it would not explain why filaments gradually become immobilized at the plateau of polymerization. Other arguments against this possibility have been summarized by Maruyama et al. (1980).]

Our results also show that, at least under some conditions, the mobile filaments initially formed in the presence of cytochalasin are gradually transformed into immobile ones without change in the mass of F-actin. The gradual immobilization seen in Figure 7 is probably due to the process of filament length redistribution—filaments slowly accumulate that are above the critical length required for network formation. However, the average filament length is probably less than that in the absence of cytochalasin, since immobilization is never as complete as in the absence of cytochalasin. Also, immobilization only puts a lower limit on averge filament length; once filaments become immobilized, further increases in length would not be detected by FPR. Our results are therefore consistent with rheological evidence (Hartwig & Stossel, 1979; MacLean-Fletcher & Pollard, 1980c) for inhibition of network formation by cytochalasin because shorter filaments will form a weaker gel.

In conclusion, the FPR data suggest that the acceleration of polymerization by cytochalasin is accompanied by a reduction in average filament size. This is consistent with the hypothesis that cytochalasin enhances nucleation of actin. The decline in filament mobility at the plateau of polymerization indicates that the short filaments initially generated by cytochalasin are gradually transformed into longer ones. This could occur if the lengthwise association of cytochalasin-free filaments is favored over the binding of cytochalasin D to the end of a filament.

Present Uncertainties in Data and Interpretation. Although the overall interpretation of our data is generally consistent with previous studies of actin polymerization, there are several remaining areas of uncertainty. One problem is that we cannot yet connect the measurements of recovery time and immobility with corresponding absolute values of filament length. This reflects the complex contributions of length, cross-linking, and concentration to the measured rates of diffusion. Studies at low concentration do not solve the problem, since both calculations and our data suggest filament interactions even at concentrations just barely adequate to induce polymerization. Nor can we achieve low concentrations by dilution, since the shear inherent in mixing would confound the interpretation by causing breaks in filaments and networks. The polydispersity of the filament population also complicates any calculation of filament length from the apparent diffusion coefficient. We have therefore emphasized relative changes in recovery times and mobility, since these changes provide much useful information without requiring oversimplified theoretical treatment of the data.

Another unresolved question is the possible effect of rotational diffusion. The laser beam is only partially depolarized, so there could be anisotropic bleaching, followed by fluorescence recovery as unbleached molecules rotate into the same orientation as the bleached molecules. We can rule out rotation around the filament's long axis because it would be too rapid to account for the observed recovery. (Making the same assumptions as we did in the calculation of the translational diffusion coefficient, we obtain a value of 10^6 s^{-1} for a 2.7-μm filament.) But rotation around the filament's short axes might occur on the same time scale as translational diffusion, since the calculated rotational diffusion coefficient is 1.1 s^{-1} (20 °C, water) for a 2.7-μm filament. [This value is extremely sensitive to length, almost to the inverse third power, for long prolate ellipsoids (Tanord, 1961).] Because the filament length is comparable to the beam size (Gaussian radius = 1.8 μm), sections of filaments would be differentially bleached according to their distance from the beam center, even in the absence of polarization; partial fluorescence recovery would then occur due to rotation of filaments into different relative orientations in the beam. Although we cannot rigorously exclude this possibility, it seems unlikely as an explanation for our results. As we indicated earlier, rotational diffusion about the filament's short axes would be far more hindered than translational diffusion parallel to the filament's long axis under the "crowded" conditions that prevail in solutions of F-actin [see Schurr (1976) and Lee et al. (1977) for further analysis of this problem]. Hence, by the time filaments were long enough to rotate on the time scale of the observed recoveries, they would be prevented from doing so by other filaments. Also, our conclusions concerning network formation and relative filament shortening under some conditions would be the same whether immobility represents prevention of rotation or prevention of translation—in either case, longer filaments form networks and do not diffuse.

Conclusions. Using FPR, we have observed several different stages of the polymerization of actin, the process of network formation, and filament length redistribution following polymerization with cytochalasin D. Future FPR studies can be done on reconstituted cytoskeletal systems in vitro with fluorescently labeled proteins. The technique can also be used to study actin filaments and networks in vivo.

Acknowledgments

We thank Dr. Elliot Elson for the use of the FPR apparatus and for helpful discussions. We thank Dr. Nils Petersen for advice on experiments, Stephen Felder for experimental advice and listings of the curve-fitting programs, and Bill Daily for advice and for the rhodamine-labeled insulin.

References

Axelrod, D., Koppel, D. E., Schlessinger, J., Elson, E., & Webb, W. W. (1976) *Biophys. J. 16*, 1055.

Bevington, P. R. (1969) *Data Reduction and Error Analysis for the Physical Sciences*, McGraw-Hill, New York.

Bloomfield, V. A. (1981) *Annu. Rev. Biophys. Bioeng. 10*, 421.
Brenner, S. L., & Korn, E. D. (1980) *J. Biol. Chem. 255*, 841.
Carlson, F. D., & Fraser, A. B. (1974) *J. Mol. Biol. 89*, 273.
Clarke, M., & Spudich, J. A. (1977) *Annu. Rev. Biochem. 46*, 797.
Dancker, P., & Low, I. (1979) *Z. Naturforsch., Biosci. 34C*, 555.
Flory, P. J. (1953) *Principles of Polymer Chemistry*, Cornell University Press, Ithaca, NY.
Fujime, S. (1970) *J. Phys. Soc. Jpn. 29*, 751.
Fujime, S., & Ishiwata, S. (1971) *J. Mol. Biol. 62*, 251.
Garcia de la Torre, J., & Bloomfield, V. A. (1981) *Q. Rev. Biophys. 14*, 81.
Gethner, J. S., & Gaskin, F. (1978) *Biophys. J. 24*, 505.
Hanson, J., & Lowy, J. (1963) *J. Mol. Biol. 6*, 46.
Hartwig, J. H., & Stossel, T. P. (1979) *J. Mol. Biol. 134*, 539.
Howard, T. H., & Lin, S. (1979) *J. Supramol. Struct. 11*, 283.
Icenogle, R. D. (1981) Ph.D. Dissertation, Cornell University, Ithaca, NY.
Kawamura, M., & Maruyama, K. (1970) *J. Biochem. (Tokyo) 67*, 437.
Koppel, D. E., Axelrod, D., Schlessinger, J., Elson, E. L., & Webb, W. W. (1976) *Biophys. J. 16*, 1315.
Lanni, F., Taylor, D. L., & Ware, B. R. (1981) *Biophys. J. 35*, 351.
Lee, W. I., Schmitz, K. S., Lin, S.-C., & Schurr, J. M. (1977) *Biopolymers 16*, 583.
MacLean-Fletcher, S. D., & Pollard, T. D. (1980a) *J. Cell Biol. 85*, 414.
MacLean-Fletcher, S., & Pollard, T. D. (1980b) *Biochem. Biophys. Res. Commun. 96*, 18.
MacLean-Fletcher, S., & Pollard, T. D. (1980c) *Cell (Cambridge, Mass.) 20*, 329.
Maeda, T., & Fujime, S. (1977) *J. Phys. Soc. Jpn. 42*, 1983.
Maruyama, K. (1964) *J. Biochem. (Tokyo) 55*, 277.
Maruyama, K., Kaibara, M., & Fukada, E. (1974) *Biochim. Biophys. Acta 371*, 20.
Maruyama, K., Hartwig, J. H., & Stossel, T. P. (1980) *Biochim. Biophys. Acta 626*, 494.
Mihashi, K. (1964) *Arch. Biochem. Biophys. 107*, 441.
Newman, J., & Carlson, F. D. (1980) *Biophys. J. 29*, 37.
Newman, J., Swinney, H. L., & Day, L. A. (1977) *J. Mol. Biol. 116*, 593.
Oosawa, F. (1980) *Biophys. Chem. 11*, 443.
Oosawa, F., & Asakura, S. (1975) *Thermodynamics of the Polymerization of Protein*, Academic Press, New York.
Pollard, T. D., & Mooseker, M. S. (1981) *J. Cell Biol. 88*, 654.
Schliwa, M. (1981) *Cell (Cambridge, Mass.) 25*, 587.
Schurr, J. M. (1976) *Q. Rev. Biophys. 9*, 109.
Tait, J. F., & Frieden, C. (1982) *Arch. Biochem. Biophys. 216*, 133.
Tanford, C. (1961) *Physical Chemistry of Macromolecules*, Wiley, New York.
Tellam, R., & Frieden, C. (1982) *Biochemistry 21*, 3207.

Raman Spectroscopic Study of the Interaction between Sulfate Anion and an Imidazolium Ring in Ribonuclease A†

Issei Harada,*,‡ Takahisa Takamatsu, Mitsuo Tasumi, and Richard C. Lord*

ABSTRACT: Raman spectra of ribonuclease A in D_2O solution at various pD values have been studied with special attention to the N-deuterated imidazolium ring vibration at 1408 cm^{-1}, the SO_4^{2-} symmetric stretching vibration at 984 cm^{-1}, the amide I′ band, and the tyrosine doublet. Concomitant decrease and increase in the intensities of the 1408- and 984-cm^{-1} bands in the pD range between 5 and 7 indicate that a sulfate anion is actually hydrogen bonded to an imidazolium ring of a histidine residue located in the interior of the molecule. The mechanism of the sulfate desorption has been compared with that on heat denaturation.

Sulfate anion is known to locate immediately adjacent to His-12 and His-119 (Wyckoff et al., 1970; Richards & Wyckoff, 1971) and stabilize the native structure of ribonuclease (Ginsberg & Carroll, 1965; Von Hippel & Wong, 1965; Winchester et al., 1970). Commercial ribonuclease A (RNase A) often contains an excess amount of sulfate anion, and the Raman spectrum of its aqueous solution gives a strong and sharp band at 984 cm^{-1} due to the symmetric stretching vibration of the anion (Lord & Yu, 1970). When the solution is heated, the intensity of the 984-cm^{-1} band increases. If the heat-denatured material is kept for a long time at elevated temperature (>70 °C) and is then cooled to room temperature, the intensity of the sulfate band remains essentially constant. If, however, the cooling process is begun shortly after the system reaches 70 °C, the sulfate band intensity decreases reversibly (Chen & Lord, 1976). Chen and Lord interpreted these results in the following way. In the course of binding to one of the histidines in RNase, the sulfate anion is converted in effect to HSO_4^- which does not give a Raman band at 984 cm^{-1} but gives two weaker bands at 895 and 1053 cm^{-1}. When the enzyme is heated, some of the bound sulfate anion is released, and the 984-cm^{-1} band increases in intensity. Irreversible denaturation by heat impairs the ability of the protein to bind sulfate anion strongly.

In order to test this proposal, it is useful to study the pH dependence of the sulfate band and that of a vibration due to imidazolium ring at the same time. Deprotonation of the

† From the Department of Chemistry, Faculty of Science, The University of Tokyo, Bunkyo-ku, Tokyo 113, Japan (I.H., T.T., and M.T.), and the Department of Chemistry and Spectroscopy Laboratory, Massachusetts Institute of Technology, Cambridge, Massachusetts 02139 (R.C.L.). *Received December 16, 1981; revised manuscript received March 29, 1982.* This work was supported in part by U.S. National Science Foundation Grant 8113662-CHE.

‡ Present address: Pharmaceutical Institute, Tohoku University, Aobayama, Sendai 980, Japan.

0006-2960/82/0421-3674$01.25/0